

Optimizing Speculative Decoding for Serving Large Language Models Using Goodput

Xiaoxuan Liu¹ Cade Daniel² Langxiang Hu³ Woosuk Kwon¹ Zhuohan Li¹ Xiangxi Mo¹
Alvin Cheung¹ Zhijie Deng⁴ Ion Stoica¹ Hao Zhang³
¹UC Berkeley ²Anyscale Inc. ³UCSD ⁴SJTU

Abstract

Reducing the inference latency of large language models (LLMs) is crucial, and speculative decoding (SD) stands out as one of the most effective techniques. Rather than letting the LLM generate all tokens directly, speculative decoding employs effective proxies to predict potential outputs, which the LLM then verifies without compromising the generation quality. Yet, deploying SD in real online LLM serving systems (with continuous batching) does not always yield improvement – under higher request rates or low speculation accuracy, it paradoxically *increases* latency. Furthermore, there is no best speculation length work for all workloads under different system loads. Based on the observations, we develop a dynamic framework SmartSpec. SmartSpec dynamically determines the best speculation length for each request (from 0, i.e., no speculation, to many tokens) – hence the associated speculative execution costs – based on a new metric called *goodput*, which characterizes the current observed load of the entire system and the speculation accuracy. We show that SmartSpec consistently reduces average request latency by up to 3.2× compared to non-speculative decoding baselines across different sizes of target models, draft models, request rates, and datasets. Moreover, SmartSpec can be applied to different styles of speculative decoding, including traditional, model-based approaches as well as model-free methods like prompt lookup and tree-style decoding.

1 Introduction

Latency is critical when deploying Large Language Models (LLMs) for online services such as search engines [25, 32], chatbots [30], and virtual assistants [27, 38, 39]. However, LLM generation is inherently slow due to its autoregressive nature, where each generated token depends on all preceding tokens. This sequential data dependency restricts tokens to be generated one by one, resulting in slow generation speeds.

Speculative decoding aims to solve the problem by employing lightweight proxies, such as a small draft model [18, 20, 24, 26, 46] or additional model heads [4, 21, 22, 43], generating multiple tokens which are then verified by the main/target LLM in parallel. Speculative Decoding can reduce the generation latency mainly for two reasons. First, the efficient proxy is much faster to run compared with running a single forward pass on the target model and hence it can generate tokens much quicker. Moreover, the verification of the draft

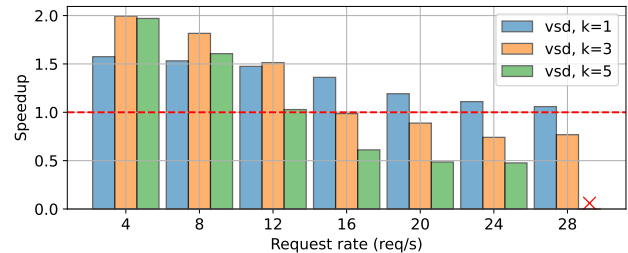


Figure 1. Speedup of vanilla speculative decoding (VSD) with proposed length $k = 1, 3, 5$ on a LLaMA-7B model with fixed input/output length = 128. We also fix the token acceptance rate to 0.7. We use LLaMA-160M as the draft model and conduct experiments on a single A100-80G. The red cross indicates the setting runs out of GPU memory and triggers swapping.

model is done in a single forward pass. Such verification is only *marginally* slower compared to letting LLM generate one new token, but it allows LLM to potentially generate *multiple* new tokens (if the guessed tokens are correct), or at least enable LLM to generate one new token (if all guessed tokens are incorrect).

While SD has demonstrated promise in accelerating single-request inference (i.e., batch size = 1), integrating it into online serving systems poses significant challenges. In real-world applications, systems batch multiple tokens to achieve high GPU utilization and SD is less efficient or can even *increase* the query latency as shown in Fig. 1. This increase is primarily due to the additional computational overhead of running the proxy models and verifying tokens that are ultimately not accepted. Whether the extra computational work translates into actual latency reduction depends on two key factors: the speculation accuracy of each request and the current load of the serving system.

First, when the majority of proposed tokens are accepted (i.e., there is a high token acceptance rate), speculative decoding can provide significant speedup, provided that the proxy model operates efficiently. Conversely, if the token acceptance rate is low, speculative decoding can introduce additional overhead rather than accelerating the process. In such cases, the main model ends up regenerating most of the tokens, rendering the proxy model’s computations superfluous and potentially slowing down the overall system.

Second, due to the inherent imperfection in speculation accuracy, speculative decoding inevitably expends some computational resources on tokens that are not ultimately accepted. Under low system load, this waste of compute is tolerable. However, under high system load conditions—where the system approaches its computational capacity and processes large batch sizes—the availability of surplus compute for speculation is greatly reduced. In such scenarios, it is more effective to allocate the limited computational resources directly to normal token generation rather than continuing to speculate, thereby minimizing the risk and maximizing the use of available compute.

Ideally, speculative decoding should be performed in an adaptive and automatic way, which can be likened to the adaptive streaming techniques used in video delivery systems. In scenarios with few users, the system can afford to engage in “high-resolution” speculative decoding, akin to streaming high-resolution video, where it utilizes abundant computational resources to make more extensive predictions per request. Conversely, as user demand increases and system resources become strained, the system shifts to “low-resolution” speculative decoding. This strategy, much like reducing video resolution during peak traffic, involves making fewer predictions per request to conserve resources while maintaining overall system functionality.

Despite its widespread recognition, speculative decoding has not yet been effectively integrated into production-level serving systems. Most prior research has explored speculative decoding with a batch size of one [4, 20]. Recent studies have extended this investigation to larger batch sizes, but these techniques have been tested primarily on relatively small LLMs [35] or in offline settings [37].

In this work, we integrate speculative decoding into a production-level serving system vLLM [19], marking the first such integration to the best of our knowledge. We also explore the trade-offs between speculation cost and decoding accuracy under varying system loads. A key innovation in our system is the introduction of a metric called “goodput,” defined as the rate of generated tokens per second. Unlike throughput, goodput in the context of speculative decoding measures only those tokens that are both verified and generated by the target model. This reflects a crucial distinction – not all output tokens qualify as generated tokens.

Goodput is an essential metric for determining the extent of speculation. It is derived from two factors: the token acceptance rate and the batch size, with the latter indicating system load. This metric adheres to two core principles. First, it limits speculation under constrained computational resources to maximize system efficiency. For example, under extremely high system loads, goodput would automatically turn off speculation to avoid wasting any compute resources. Second, this metric increases the proposed length for requests that are easy to predict, as indicated by the high token acceptance rate in previous generation steps. By leveraging

the predictability of these queries, the system can enhance overall performance.

However, we cannot measure goodput directly because the decision needs to be made before knowing the goodput. We must determine the proposed length and which requests to run (batch size) based on an estimate of goodput, as these two factors influence its value. To estimate goodput, we predict the accepted token length for all requests within a single generation step using the token acceptance rate. A simple linear model is then employed to estimate the batch execution time. By combining the predicted token length and execution time, we can approximate goodput.

Leveraging goodput, we developed the dynamic speculative decoding framework SmartSpec. SmartSpec dynamically modulates each request’s speculation length – from no speculation (i.e., zero) to many tokens – based on the estimated *goodput*, adjusting speculation intensities to ensure consistent reduction (instead of increase) of the request latency. SmartSpec also accommodates various speculative decoding methods, including draft model-based approaches and model-free techniques such as prompt lookup [33] and tree-based decoding [4]. Accommodating diverse SD methods is crucial because different techniques are suited to different workloads. For instance, prompt lookup decoding is more beneficial for summarization tasks, while tree-based approaches like Medusa are more useful for online chatting. For all SD methods evaluated across all datasets, SmartSpec guarantees improved performance without any degradation, which is a crucial feature for making SD useful in a production-ready online serving system.

In summary, the paper makes the following contributions:

- We perform the first study on speculative decoding within a real-world, online serving system with continuous batching scheduling (§3).
- We define the goodput for speculative decoding, which takes into account both system throughput and speculation accuracy (§4).
- We design and implement a speculative decoding scheduling framework that utilizes goodput as key metrics to determine the optimal proposal length for different request volumes (§5, §6). Evaluation of SmartSpec on five models across different tasks shows that SmartSpec consistently reduces latency under different system loads, bringing up to 3.2× latency reduction compared with non-speculative decoding baseline (§7).

2 Background

Given a list of tokens (x_1, \dots, x_n) , a large language model (LLM) [1, 3] is trained to predict the conditional probability distribution for the next token: $P(x_{n+1} | x_1, \dots, x_n)$. When deployed as a service [19, 31], the LLM takes in a list of

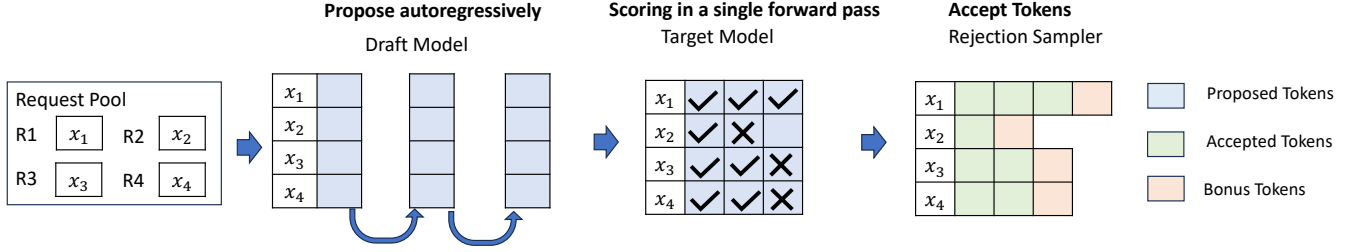


Figure 2. A single generation step when combining continuous batching with speculative decoding. The draft model runs in an autoregressive manner. The proposed tokens are sent to the target model for scoring in a single forward pass. A single generation step can generate more than one token for each request.

tokens from the user request and generates an output sequence $(x_{n+1}, \dots, x_{n+T})$. The generation process requires sequentially evaluating the probability and samples the token at every position for T times.

Due to the sequential data dependency, this computation often suffers from low device utilization when running on GPUs, which leads to high inference latency and low serving throughput [31]. Therefore, many previous works propose different algorithms to decrease the latency or increase the throughput when serving LLMs. In this paper, we focus on two categories of optimization algorithms, *speculative decoding* and *continuous batching*.

2.1 Speculative Decoding

Although LLMs can only generate output tokens sequentially, when facing a list of output tokens $(x_{n+1}, \dots, x_{n+T})$, LLMs can efficiently evaluate the probabilities for each token $P(x_{n+1} | x_1, \dots, x_n), \dots, P(x_{n+T} | x_1, \dots, x_{n+T-1})$ in parallel. *Speculative decoding* [5, 20] utilizes this property to reduce the generation latency of LLMs.

Specifically, in speculative decoding, we turn the target LLM into an evaluator. At every step, we use another more efficient draft model to propose a list of candidate tokens $(y_{n+1}, \dots, y_{n+k})$, where k is the number of proposed candidates. Then, we feed these k tokens to the target LLM to evaluate the probabilities $P(y_{n+1} | x_1, \dots, x_n), \dots, P(y_{n+k} | x_1, \dots, x_n, y_{n+1}, \dots, y_{n+k-1})$ in parallel. Based on the probabilities and sampling methods, we will accept a subset of tokens y_1, \dots, y_m , where m is the number of accepted tokens. As an example, for greedy sampling, we check whether each y_{n+i} is the token that maximizes the probability distribution $P(\cdot | x_1, \dots, x_n, y_{n+1}, \dots, y_{n+i-1})$ and accept the first m tokens y_1, \dots, y_m that satisfy the condition. Note that for the position $m + 1$, we can directly sample y_{m+1} from the distribution $P(\cdot | x_1, \dots, x_n, y_{n+1}, \dots, y_{n+m-1})$. Finally, we will take $m + 1$ tokens y_1, \dots, y_{m+1} as LLM outputs for this step.

Speculative decoding has two core properties: (1) Speculative decoding does not change the behavior of the LLM sampling process, and thus generates exactly the same output as vanilla decoding algorithms without any accuracy loss.

(2) The efficiency and the effective speedup of speculative decoding algorithms depend on two factors: the accuracy of the draft model matching the outputs of the target model and the efficiency of the draft model.

Many previous work focuses on improving the accuracy and efficiency of speculative decoding and can be categorized into two parts: (1) Draft LLM-based speculative decoding, which uses a small LLM as a draft model to propose candidate tokens [6, 24, 26, 40, 46]. (2) Draft-model free speculative decoding, which uses either a branch of the target model or uses other sources (e.g., from an external database) to generate the candidate tokens [4, 10, 21, 22, 33]. In this work, we study the behavior of both types of speculative decoding method.

2.2 Continuous Batching

Due to the sequential dependency, when generating output for a single output, LLMs severely under-utilize the GPUs. To increase the GPU utilization, one can batch multiple requests in one step and process them in parallel. However, batching the requests to an LLM is non-trivial: First, the requests may arrive at different times. A naive batching strategy would either make earlier requests wait for later ones or delay the incoming requests until earlier ones finish, leading to significant queueing delays. Second, the requests may have vastly different input and output lengths. A straightforward batching technique would pad the inputs and outputs of the requests to equalize their lengths, wasting GPU computation and memory.

Continuous batching [11, 41] is proposed to address this problem. Instead of batching at the request level, continuous batching batches at the step level. For each step, completed requests from previous step are removed from the batch, and newly received requests are added. Therefore, a new request can immediately start to be processed after it is received. This leads to a larger batch size at every step, which improves GPU utilization and thus the serving throughput. Moreover, with special GPU kernels, continuous batching can eliminate the need to pad requests of different lengths, which further improves the serving throughput. The technique has been

integrated in all popular LLM inference engines, such as vLLM [19] and TensorRT-LLM [29].

3 Speculative Decoding with Continuous Batching

Speculative decoding changes continuous batching by allowing each generation step to produce multiple rather than a single token per request. It utilizes a draft model to suggest a range of possible tokens for a request at each generation step. These proposed tokens for all requests are then collectively processed in a batch by the target model for verification.

Figure 4 illustrates the three phases of speculative decoding: proposal, scoring, and acceptance. In proposal, the draft model examines the request pool and generates tokens in an autoregressive manner. During scoring, all the proposed tokens are evaluated collectively in a single forward pass. After accepting the tokens with rejection sampling, each request can yield multiple tokens in a single pass. The generated tokens comprise those proposed by the draft model and subsequently accepted by the target model, plus a bonus token. This bonus token either corrects a prediction made by the draft model or is generated by the target model when it accepts all proposed tokens.

3.1 Vanilla Speculative Decoding Latency

To understand the performance implication of vanilla speculative decoding in the context of continuous batching, we conduct an analysis shown in Fig. 1, showcasing the speedup achieved under varying request rates. In this analysis, to mitigate confounding variables, we set the token acceptance rate (0.7) and standardize the input and output lengths across all requests (input length=output length=128). The results show that at a low request rate (specifically, a request rate of 4), proposing 3 or 5 tokens results in the most significant speedup. However, as the request rate increases, the advantage of proposing more tokens diminishes rapidly: when the request rate exceeds 12, proposing 5 tokens offers no performance improvements. Likewise, at a request rate greater than 16, proposing 3 tokens yields performance degradation.

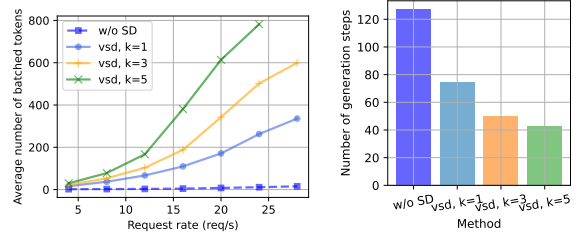
Several insights emerged from this experiment. Firstly, speculative decoding does not invariably lead to improved performance; in fact, it may detrimentally affect performance at higher request rates. Secondly, the optimal length for speculation varies with the request rate. At lower request rates, speculating more is better, but at higher request rates, it may not even make sense to speculate at all.

3.2 Latency Analysis

To understand the phenomenon, we can approximate the request latency as:

$$request\ latency \approx batch\ latency \times generation\ steps \quad (1)$$

where *batch latency* refers to the time required to process a single batch and *generation steps* is the average number



(a) Average batch size.

(b) Average number of generation steps.

Figure 3. Latency analysis: batch size and generation step.

of iterations needed for the target model to complete a request. For simplicity, we exclude the latency associated with the draft model, assume uniform latency across different generation steps, and focus solely on the *batch latency* per *generation step* incurred by the target model. Fig. 3a illustrates that proposing more tokens at each step leads to a greater accumulation of tokens within the same batch and hence higher *batch latency*. On the other hand, as shown in Fig. 3b, generating more tokens in a single forward pass of the target model reduces the number of *generation steps*. Given the approximation presented in Eq. 1, the feasibility of achieving a speedup is determined by the interplay between these two factors.

3.3 Granularity of Proposed Lengths

Lastly, continuous batching enables flexible scheduling. As shown in Fig. 4, there are three levels of granularity for proposed lengths: (1) Global: This is the simplest way to implement speculative decoding with continuous batching, where the proposed length for all requests across all generation steps is uniform. However, this approach overlooks system behavior; as previously mentioned, speculative decoding can degrade performance. (2) Step Level: Here all requests within the same batch have the same proposed length, although the length can vary between steps. This allows proposed lengths to adapt to different system loads. For instance, when the number of requests is high, the proposed length for a given step can be reduced to conserve computational resources. (3) Request Level: This is the most fine-grain level of scheduling, where each request can have its own proposed length. It allows for the prioritization of ‘easier’ requests by proposing a higher number of tokens for them, based on the assumption that it is more likely for more tokens to be generated in a single step for these requests.

In this section, we analyze the performance characteristics of naive speculative decoding with continuous batching across various request rates. We explore the reasons for performance degradation and highlight the possibility of implementing flexible scheduling. Determining the optimal proposed length to achieve minimal latency across diverse

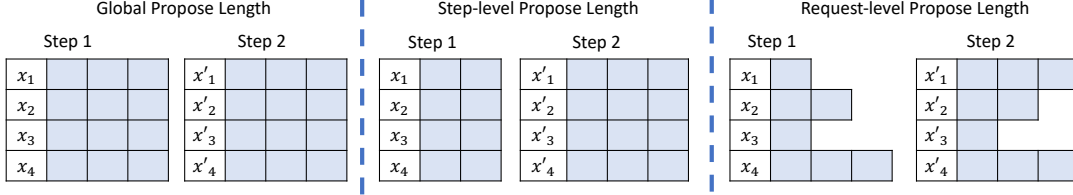


Figure 4. Flexible proposed lengths.

workloads under different request volumes is a significant challenge that we address in the following discussion.

4 The Goodput of Speculative Decoding

We now define the *goodput* of serving LLMs with speculative decoding and elaborate on how it is connected to the overall system efficiency. Then we describe how goodput can be estimated given various prediction methods on the acceptance of speculated tokens.

4.1 Defining Goodput

We define the *per-step* throughput of serving a request using an LLM as:

$$\text{Throughput} = \frac{\text{Number of Output Tokens}}{\text{Execution Time}} \quad (2)$$

Throughput refers to the output rate of tokens generated by the model per unit of time. Existing systems such as vLLM [19] and Orca [41] all aim to maximize the throughput, as doing so enhances the overall efficiency of the system.

Goodput in speculative decoding. In speculative decoding, not all tokens output by the target model in the scoring phase (Fig. 4) are guaranteed to pass through the rejection sampling mechanism. Consequently, these tokens might not represent the actual tokens generated in a single step. To address this discrepancy, we define *goodput* as:

$$\text{Goodput} = \frac{\text{Number of Generated Tokens}}{\text{Execution Time}} \quad (3)$$

Here, the goodput refers to the rate at which tokens are generated, measured in tokens per second. This includes both the proposed tokens that are subsequently accepted and the bonus tokens that the target model produces during verification.

Parameters of Goodput. While the above definition is general across different speculative decoding algorithms, we focus on three configuration parameters of particular impact in the context of speculative decoding scheduling:

1. Proposed length: the number of tokens proposed by the draft model in each step.
2. Requests to run: which request(s) to run in each step.

4.2 Understanding Goodput

Goodput, essentially defined as the ratio of expected gain to costs, offers valuable insights into how batch size and proposed length should interact to optimize system performance.

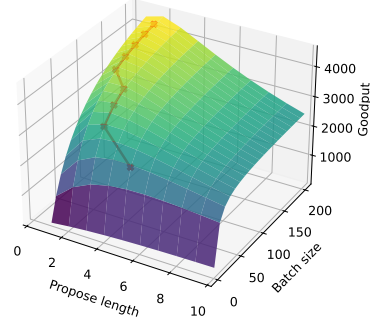


Figure 5. Goodput as a function of proposed length and batch size. We calculated the goodput using the coefficients from the A100-7B model, as detailed in Sec. 4.3. We assumed a uniform token acceptance rate of 0.7 and employed the formula described in Section 4.4 to estimate the accepted length.

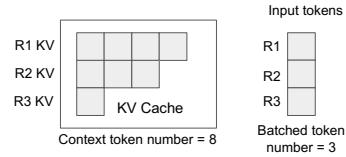


Figure 6. An example of context token number and batched token number used in modeling the forward execution time.

To demonstrate the intuition behind goodput, Fig. 5 shows the goodput values across various batch sizes and proposed lengths, assuming a uniform token acceptance rate.

Propose more for small batches. In Fig. 5, the red line indicates the optimal proposed length for each batch size. Notably, small batch sizes require proposing more than 4 tokens per per request to achieve the maximum goodput. As batch size increases, the optimal proposal length decreases.

Propose less for large batches. For large batch sizes, not speculate altogether can result in higher goodput. This occurs as the cost of unsuccessful speculations increases significantly with larger batch sizes, outpacing the potential gains.

Prefer batching over speculating. Consider a scenario where the acceptance of tokens is independent, with each token having a 0.7 probability of acceptance. In this case, the probability of accepting the first token is 0.7, while the

probability of accepting both the first and second tokens is $0.7 \times 0.7 = 0.49$. Consequently, increasing the batch size tends to produce more tokens at the same cost. Doubling the batch size results in twice the number of generated tokens, whereas doubling the proposed length does not necessarily yield a proportional increase in output.

Optimizing goodput reduces request latency. Request latency consists of the request’s queuing delay and total execution time. When the request rate is low, improving goodput effectively reduces the overall execution time by utilizing speculative decoding with an optimal proposed length. On the other hand, at high request rates, optimizing goodput helps decrease queuing delays by increasing the system’s capacity to process requests through large batch sizes and moderate speculative decoding. Overall, strategically adjusting batch sizes and proposed lengths based on goodput enables managing both high and low demand scenarios effectively.

4.3 Modeling Batch Execution Time

The batch execution time is defined as the total time required to complete a speculative decoding step, incorporating both the draft and target model execution times. This can be mathematically represented as:

$$T_{batch} = T_{draft} + T_{target} \quad (4)$$

Modeling T_{draft} and T_{target} . For draft-model-free speculative decoding, we assign a small constant factor $T_{draft} = C$. For draft model-based speculative decoding, the draft model operates in an autoregressive manner and supports continuous batching. Consequently, the total execution time for the draft model is the aggregate of the execution times across all draft steps. Each step involves a single forward pass of the draft model. Given the variability in propose lengths across different requests, the execution time per step may differ. The draft model execution time is a sum of the execution time of each forward pass:

$$T_{draft} = \sum_{i=1}^s T_{fwd}(M, N_{context}(s), N_{batched}(s)) \quad (5)$$

Here, s is the number of autoregressive steps. Concretely, $s = \max(s_1, s_2, \dots, s_n)$, where s_i is the proposed length of request i in the batch. The forward execution time, T_{fwd} , varies across different steps due to different numbers of context tokens ($N_{context}$) and batched tokens ($N_{batched}$) at each step. It also depends on the model M the forward pass is running on. These variations directly influence the duration of the forward execution time, as outlined in **Modeling T_{fwd}** . below.

The target model executes a single forward pass for its operation:

$$T_{target} = T_{fwd}(N_{context}, N_{batched}) \quad (6)$$

Modeling T_{fwd} . We then define T_{fwd} , the time for a forward pass, which is applicable to both the draft and target

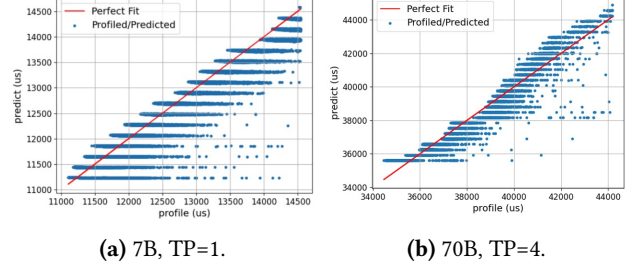


Figure 7. Predicted versus profiled batch latency. TP: tensor parallel. The x-axis represents the profiled time, while the y-axis shows the predicted execution time using Formula 7. The red line symbolizes perfect prediction, indicating where the predicted time matches the profiled time exactly.

models:

$$T_{fwd}(M, N_{context}, N_{batched}) = \alpha_M \cdot N_{context} + \gamma_M \cdot N_{batched} + \delta_M \quad (7)$$

where $N_{context}$ represents the number of context tokens within the batch and $N_{batched}$ denotes the number of batched tokens, as illustrated in Figure 7. The term $\alpha_M \cdot N_{context}$ reflects the time required to load the key-value cache, scaling linearly with the number of context tokens. The term $\gamma_M \cdot N_{batched}$ accounts for the computation time, while δ_M represents the time to load the model parameters. The coefficients α_M , γ_M , and δ_M are contingent upon the model and hardware configuration, necessitating distinct sets of $(\alpha_M, \gamma_M, \delta_M)$ for various models or hardware environments. In practical terms, we systematically profile the batch execution time for each specific model and hardware combination, and subsequently adjust the values of α_M , γ_M , and δ_M to accurately reflect these profiles.

Modeling $N_{batched}$. If at each position the proposal method suggests only one token (top 1 candidate), the number of tokens sent for verification is simply the sum of the proposed lengths of each request. For top-k tree-style speculative decoding, assuming full tree verification, assume full tree verification, there are H heads and we propose k_i tokens for head i , the number of batched tokens is $\sum_{h=1}^H \prod_{i=1}^h k_i$ [4]. Figure 8 illustrates an example of the number of batched tokens in Medusa. As shown, one characteristic of full tree speculative decoding is its high cost. In the example, even if a maximum of four tokens can be accepted (three proposed tokens plus one bonus token), a total of 27 tokens are sent for verification. This can be problematic for large batch sizes. Smarter methods to construct the tree, such as those proposed by [6] and SmartSpec, are needed to make topk candidate speculative applicable in a real serving system.

Validating performance model. Figure 7 illustrates the application of our T_{fwd} function, designed to estimate batch

execution times. This is demonstrated under a uniform workload condition, where each request maintains identical input/output sizes (input length = output length = 128). Furthermore, we adjust the request rates to evaluate the function’s performance across a spectrum of batch sizes, with each data point representing an execution step. Our analysis encompasses comparisons between models of 7B and 70B parameters, employing tensor parallelism settings of 1 and 4, respectively. Overall, the results demonstrate that our model accurately captures the trends present in the observed data, effectively adapting to variations in request rates, model sizes, and levels of parallelism.

4.4 Modeling Generated Length

To accurately predict goodput, as defined in Equation 3, our methodology necessitates modeling the number of tokens produced during each generation step. The capability to accurately predict the length of generated content is crucial for minimizing computational waste and enhancing the efficiency of scheduling, as the predictions directly influence the determination of the proposed length for generation and the subsequent scheduling decisions. SmartSpec explores three methods to model the accepted length.

Top1 candidate generated length. SmartSpec employs a moving average method to estimate the token acceptance rate for specified pairs of draft and target on a given dataset. Concretely, SmartSpec records the token acceptance rate from previous generation steps. For predicting the rate in the current step, it calculates the average from these past rates. The moving average method used requires a window size; however, we find that the performance is relatively insensitive to the choice of this window size. This approach presupposes uniform token acceptance behavior across diverse requests. The acceptance length is predicted using the formula introduced in the original speculative decoding paper [20].

$$l(\alpha, k) = \frac{1 - \alpha^{k+1}}{1 - \alpha} \quad (8)$$

In this context, l represents the generated length for each request, inclusive of the bonus token. The variable α denotes the average token acceptance rate observed within the calibrated dataset, while k corresponds to the number of tokens proposed. We can then write out the total number of generated tokens in a single batch:

$$\text{generated tokens} = \sum_{i \in R} \frac{1 - \alpha_i^{k_i+1}}{1 - \alpha_i} \quad (9)$$

Here, we can have different granularity of token acceptance rate. (1) Global token acceptance rate: it is assumed that each request exhibits identical acceptance behavior. Consequently, different requests within the same batch share the same token acceptance rate and proposed length, $k_1 = k_2 = \dots = k_n$, $\alpha_1 = \alpha_2 = \dots = \alpha_n$. (2) Request level token acceptance rate: individual requests exhibit distinct acceptance rates (α s)

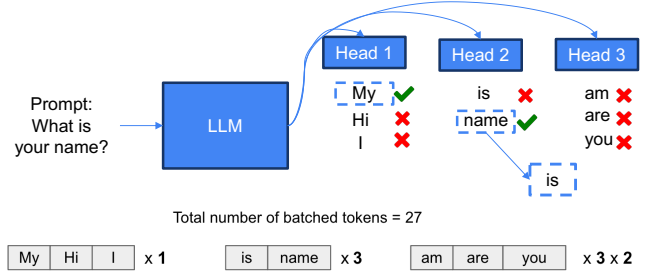


Figure 8. An example Medusa-style speculative decoding utilizing three distinct heads. Each head is tasked with generating proposals for one position. In this scenario, the first head proposes the top three most likely tokens, the second head selects the top two, and the third head also chooses the top three. During this forward run, three tokens [‘My’, ‘name’, ‘is’] are generated – two from the proposals plus one bonus token. Collectively, this setup represents a total of 18 (3x2x3) possible continuations.

and proposed lengths (k s) due to varying levels of difficulty, necessitating the proposal of a differing number of tokens for each.

Topk tree-style generated length. In tree-style speculative decoding, we can have multiple candidates for the same position. In Medusa, each head is responsible for proposing for a position. Figure 8 shows an example, where there are three candidates for position 1, two candidates for position 2, and three candidates for position 3.

To estimate the accepted length, we make the following assumptions: 1. The token acceptance rate for each proposed token at head i is denoted as α_i . All tokens within the top- k share the same token acceptance rate. 2. The acceptance behavior is independent across different heads; that is, the acceptance of a token at head i does not influence the acceptance of a token at head $i + 1$. Suppose there are h heads, and we propose k_1, k_2, \dots, k_h tokens for heads 1, 2, \dots , h , respectively. The token acceptance rates for these heads are $\alpha_1, \alpha_2, \dots, \alpha_h$. For simplicity in the formula below, we define $\alpha_{h+1} = 0$. The expected accepted length given the structure can be formulated as:

$$l(\alpha_1 \dots \alpha_h, k_1 \dots k_h) = \sum_{i=1..h} (i+1) \times (1 - \alpha_{i+1}) \times \prod_{j=1..i} [1 - (1 - \alpha_j)^{k_j}] \quad (10)$$

Here, $(1 - \alpha_{i+1}) \times \prod_{j=1}^i [1 - (1 - \alpha_j)^{k_j}]$ represents the probability of accepting $(i + 1)$ tokens, where the “+1” accounts for the bonus token. To understand this probability, it hinges on two conditions: (1) At least one token is accepted from heads 1 through i . (2) None of the proposed tokens at head $i + 1$ are accepted. Thus, the probability is calculated as the product of the probabilities of conditions (1) and (2).

Since SmartSpec is a versatile speculative decoding framework, users can integrate various estimation methods, such

as the confidence-based method discussed in the Appendix. Additionally, users may even employ machine learning models for predictions. We leave it as future work to develop an accurate and efficient predictor for accepted length.

5 Serving Requests Using SmartSpec

We now describe the flow of a single decoding step outlined in Algorithm 2. Initially, we enumerate potential requests for a single batch (line 2). SmartSpec uses a first-come, first-served strategy. Assuming n requests in the pending batch, we construct candidate batches by selecting prefixes of increasing length: batches with 1 request, 2 requests, etc., up to n requests. For each potential batch, we use goodput to determine the optimal proposed length (line 4). Additionally, we verify if there is sufficient space in the KV cache (lines 5-7). For Top-1 candidate speculative decoding, SmartSpec will determine the optimal proposed length. For Top-k tree-style speculative decoding, SmartSpec will identify the optimal Top-k value for each proposal head. In both cases, the token acceptance rate is factored into Eqn. 8 to calculate the estimated generation length. SmartSpec then uses this estimated length along with Eqn. 3 and a performance model (elaborated in Sec. 4.3) to estimate goodput. After identifying the optimal proposed lengths or Top-k value, SmartSpec executes these steps sequentially. For draft-model based speculative decoding, the proposal phase operates in an autoregressive manner and incorporates continuous batching (line 12). Then SmartSpec verifies the proposed tokens and records the token acceptance rate of current step (line 13).

To estimate the current token acceptance rate, SmartSpec records the acceptance rate from previous scoring steps (line 13 in Alg. 2) and computes the moving average of these rates (lines 5-8 in Alg. 1). Although moving average is an imperfect estimator for token acceptance rate, goodput remains robust and results in latency reduction to be discussed in Sec. 7.2.1. **Prefill disabling.** In draft-model based speculative decoding, the prefill phase of the running draft model can introduce overhead, especially when request rate is high. By default, speculative decoding is disabled during the prefill phase. However, to synchronize the KV cache between the draft and target models, the system still executes the draft model’s prefill phase by default, even if no tokens are subsequently proposed by SmartSpec. This can lead to the wasteful consumption of memory and computational resources. To address this issue, we use a feedback-based method that automatically disables the draft model’s prefill run. For each generation step, SmartSpec records the proposed length. During each prefill phase, SmartSpec checks the proposed length from previous decoding steps. If the percentage of times no tokens were proposed exceeds a predefined threshold, SmartSpec will disable the draft model’s prefill run for the current request and classify the request as non-speculative. Since the draft model’s KV cache is not maintained for these

Algorithm 1 Goodput Estimation for Step-level Proposed Length

Require: Proposed length k for all requests in the batch for Top-1 candidate speculative decoding. Number of sampled tokens $k_1 \dots k_h$ for each head for Top-k tree-style speculative decoding. Estimation method $Method$. Token acceptance rate $prev_alphas$ of previous steps. All requests in the batch R .

```

1:  $n \leftarrow len(R)$ 
2: if  $Method ==$  Top-1 candidate speculative decoding then
3:    $\alpha \leftarrow MovingAvg(prev\_alphas)$ 
4:    $generated\_len = n \times \frac{1-\alpha^{k+1}}{(1-\alpha)} \times n$ 
5:    $batch\_execution\_time = T(R, [k])$ 
6: else if  $Method ==$  Top-k tree-style speculative decoding then
7:    $\alpha_1, \alpha_2 \dots \alpha_h \leftarrow MovingAvg(prev\_alphas)$ 
8:    $generated\_len = n \times \sum_{i=1..h} (i+1) \times (1-\alpha_{i+1}) \times \prod_{j=1 \dots i} [1 - (1-\alpha_j)^{k_j}]$ 
9:    $batch\_execution\_time = T(R, [k_1, k_2 \dots k_h])$ 
10: end if
11: return  $\frac{generated\_len}{batch\_execution\_time}$ 
```

Algorithm 2 SmartSpec token acceptance rate based proposal and verification.

Require: Pending requests R . Max proposed length V . Token acceptance rates of previous decoding steps $prev_alphas$.

```

1:  $best\_goodput, best\_proposed\_lens \leftarrow -1, []$ 
2:  $batch\_candidates \leftarrow GetBatchCandidates()$ 
3: for  $batch$  in  $batch\_candidates$  do
4:    $cur\_goodput, cur\_proposed\_lens \leftarrow$ 
      $Argmax_{k_1, k_2 \dots k_n} (Goodput(k_1, k_2 \dots k_n, prev\_alphas))$ 
5:   if not  $HasSlot(batch)$  then
6:     continue.
7:   end if
8:   if  $cur\_goodput > best\_goodput$  then
9:      $best\_goodput, best\_proposed\_lens \leftarrow$ 
        $cur\_goodput, cur\_proposed\_lens$ 
10:  end if
11: end for
12:  $Propose(R, best\_proposed\_lens)$ 
13:  $\alpha_{cur} = Score(R, best\_proposed\_lens)$ 
14:  $prev\_alphas.append(\alpha_{cur})$ 
```

requests, speculative decoding is also disabled for all subsequent decoding steps for these requests. The threshold for disabling the prefill run is adjustable, allowing users to tailor the level of conservative speculative decoding to their needs. Empirically, setting this threshold to 0.7 has yielded good performance, balancing resource efficiency with decoding effectiveness.

Discussion and Complexity Analysis. For each batch, the overhead of SmartSpec consists of three components: accepted length estimation, batch execution time modeling, and goodput-guided proposal length optimization. Computing accepted length and batch execution time are $O(1)$, as

they use moving average based token acceptance rate and offline profiled model coefficients, as detailed in Secs. 4.4 and 4.3.

The complexity of goodput-guided optimization varies depending on whether it utilizes request-level or global token acceptance rates. In this work, we empirically find that both granularities yield similar performance gains. However, given that the request-level token acceptance rate introduces significant engineering complexity, we opt to use the global token acceptance rate to estimate the accepted length. Since the maximum proposed length V is typically less than 10, we can efficiently enumerate all possible proposed lengths to find the one that maximizes goodput. This is a very small overhead in comparison with LLM forward pass: let s be the sequence length, ℓ be number of decoder layers in the model, h be the hidden dimension size, n be the batch size, each forward pass’s complexity is at the order of $O(\ell n(sh^2 + s^2h)) \gg O(nV)$.

6 System Design and Architecture

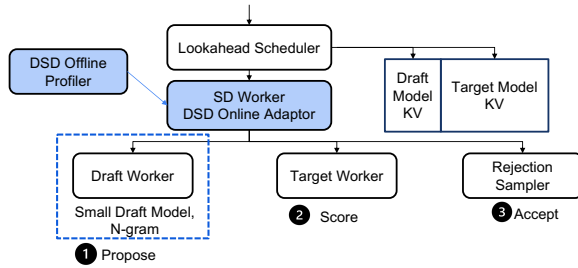


Figure 9. System architecture of SmartSpec in vLLM.

We implement SmartSpec within vllm [19] and illustrate the system architecture in Figure 9. Initially, upon receiving a request, the lookahead scheduler takes charge. This scheduler is tasked with dispatching requests for immediate execution and managing resource allocation within the key-value (KV) cache. It is termed a "lookahead" scheduler because it proactively reserves multiple KV cache spots for tokens that have yet to be generated. Subsequently, the engine forwards these active requests to the speculative decoding worker, which, in turn, activates the draft worker. The draft worker operates the draft model through several steps, each generating a proposed token. It offers a standardized interface that supports various speculative decoding approaches, such as a small draft model or an n-gram model. Subsequently, the target worker utilizes the target model for scoring and verification purposes. Note here both the draft and target models interact with the KV cache during their forward.

For effective memory management within speculative decoding, it is essential to maintain the key-value (KV) cache for both the draft and target workers. In scenarios where draft-model-based speculative decoding is employed, we divide the total memory allocated for the KV cache into two

distinct segments: one dedicated to the draft model and the other to the target model. Our observations have consistently shown that the number of required slots for both the draft and target models remains constant both before and after the execution step. Consequently, we allocate the KV cache to provide an equal number of slots for each model, with the scheduler assigning the same number of slots to both models. This approach not only simplifies the system’s architecture but also reduces its complexity. On the other hand, when carrying out draft-model free speculative decoding, SmartSpec maintains the KV cache as it without speculative decoding.

To dynamically adjust the proposed length, we employ the online adaptor in conjunction with the offline profiler. The offline profiler is responsible for analyzing both the draft (if any) and target models to derive the performance coefficients critical for the performance model, as detailed in Section 4.3. These coefficients are subsequently utilized by the online adaptor, which aggregates batch information. Based on this data, the online adaptor adjusts the proposal length for the draft worker and the verification length for the target model.

7 Evaluation

Model and server configurations. We test on two popular open source model families: Llama and Mistral. For Llama, we use Vicuna-7B-v1.5, Vicuna-33B-v1.3 [44], and Llama-2-70b-chat-hf [36]. For Mistral, we use Mistral-7B-Instruct-v0.1 [13] and Mixtral-8x7B-Instruct-v0.1 [14]. We use a single A100-80G [28] GPU for the 7B model, 4×A100-80G GPUs for the 33B model, and 8×A100-80G GPUs for the 70B model. For the draft model-based method, the draft model operates with tensor parallelism set to 1, and only the target model is sharded across multiple GPUs. We provide detailed specifications of the setup in Table 1.

Evaluated methods and baselines. We test the efficiency of SmartSpec on both standard speculative decoding, where a draft model is used to make the proposal, and prompt lookup decoding, where the proposal is made by looking up ngrams in the prompt. Both mechanisms are detailed in Sec. 2.1. For standard speculative decoding, we fine-tune Llama-160M on the shareGPT dataset to improve its general proposal capability and use it as the draft model for Vicuna-7B. For Llama2-70B model, we use Vicuna-7B as the draft. For all the settings, the draft model shares the same tensor parallel degree as the target model.

We compared SmartSpec against two baselines: vanilla auto-regressive inference, which does not incorporate speculative decoding, and using speculative decoding with a fixed proposed length of 1, 3, and 5 across all execution steps.

Workloads. In our study, we focus on four types of workloads, online chatting, text-to-SQL, summarization, and question answering given context. For online chatting, we utilize datasets from ShareGPT [2], Chatbot Arena [44]. For text-to-SQL, we use the spider [42] dataset. For summarization and

Task	Dataset	SD Method	Draft Model (TP)	Target Model (TP)	Hardware (Total Mem.)
Online Chatting	Arena[44]	VSD[20]	Llama-160M(1)	Vicuna-7B(1)	A100 (80G)
			Llama-160M(1)	Vicuna-33B(4)	4×A100 (320G)
			TinyLlama-1.1B (1)	Llama2-70B (8)	8×A100 (640G)
Llama-160M(1)	Vicuna-7B(1)		A100 (80G)		
Llama-160M(1)	Vicuna-33B(4)		4×A100 (320G)		
TinyLlama-1.1B (1)	Llama2-70B (8)		8×A100 (640G)		
Tex-to-SQL	Spider[42]	PTL[33]	Llama-160M(1)	Vicuna-7B(1)	A100 (80G)
Summarization	CNN/Daily Mail[12, 34]		Llama-160M(1)	Vicuna-33B(4)	4×A100 (320G)
			None	Mistral-7B (1)	A100 (80G)
Context QA	HAGRID[16]		None	Mixture-8×7B (8)	8×A100 (640G)
			None	Mistral-7B (1)	A100 (80G)
None	None		None	Mixture-8×7B(8)	8×A100 (640G)

Table 1. Dataset, model and server configuration. VSD: Vanilla speculative decoding. PTL: Prompt lookup decoding.

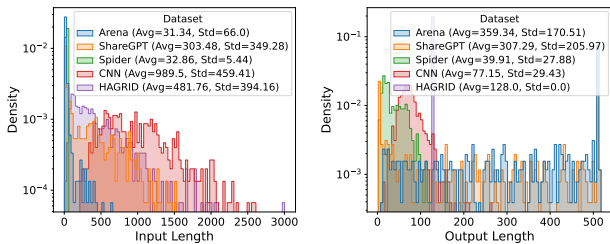


Figure 10. Input/Output length distributions.

question answering, we use the original dataset CNN/Daily Mail [34] and HAGRID [16] from the prompt lookup decoding work. We show the workload characteristics (average input length and average output length) in Fig. 10. For online chatting, the input is of medium length while the output length is longer and show higher variance. For summarization and question answering, the input length is long and the output is short. For the question answering, since we do not have the ground truth in the dataset, we set a fixed output length 128. For all workloads, we generate request arrival times using Poisson distribution with different request rates. We use greedy sampling for all served requests.

7.1 Latency Measurement

We first evaluate the effectiveness of SmartSpec in reducing request latency for both draft model-based and draft model-free speculative decoding.

7.1.1 Draft-model based speculative decoding. We evaluated the average request latency across different datasets, focusing on the performance of SmartSpec in comparison to baseline strategies in Figs. 11 and 12. In environments with a low request rate, SmartSpec demonstrates performance similar to that from greedily predicting a higher number of tokens (e.g., $k = 3$ or 5) to maximize speedup. This similarity suggests that SmartSpec predicts just enough tokens under light loads to effectively reduce request latency through speculative decoding. However, on a few occasions when request

rates are low, there are slight performance differences between SmartSpec and standard SD. In those cases, standard SD, which predicts a higher number of tokens, marginally outperforms SmartSpec with a more pronounced speedup. This discrepancy can be attributed to our imperfect acceptance length predictor, resulting in standard SD with a longer proposed length performing better as more tokens could potentially be accepted.

Conversely, in scenarios with a high request rate, the system’s performance mirrors situations where no tokens are predicted, effectively indicating that speculative decoding is disabled under conditions of high request volume. It is important to note that in this regime, the latency associated with using standard SD and proposing high numbers of tokens escalates rapidly, leading to significant performance degradation. This is exemplified in Fig. 11 (c) when the request rate is at 32 and (f) when the request rate exceeds 5.

In cases such as Fig. 11 (d) and (e), the relative speedup for these baselines rebounds after initially dropping when the request rate exceeds 2. This rebound occurs because, as the request rate continues to increase, it reaches a point where even baseline decoding without speculation begins to suffer from queuing delays. This phenomenon relatively improves the speedup of standard SD baselines, despite them experiencing higher overall latencies.

In general, speculative decoding is most effective when the system has sufficient computational resources: the larger the model, the smaller the request rate region where we see speedup from speculation. This is expected as speculative decoding requires additional computational power; when the model is large and computational resources do not scale proportionally, the system is likely to be compute-bound. This underscores the importance of SmartSpec. It is crucial for SmartSpec to consistently match or outperform the established baseline across different scenarios. This characteristic is vital for implementing speculative decoding techniques in real production environments, as it ensures that adopting

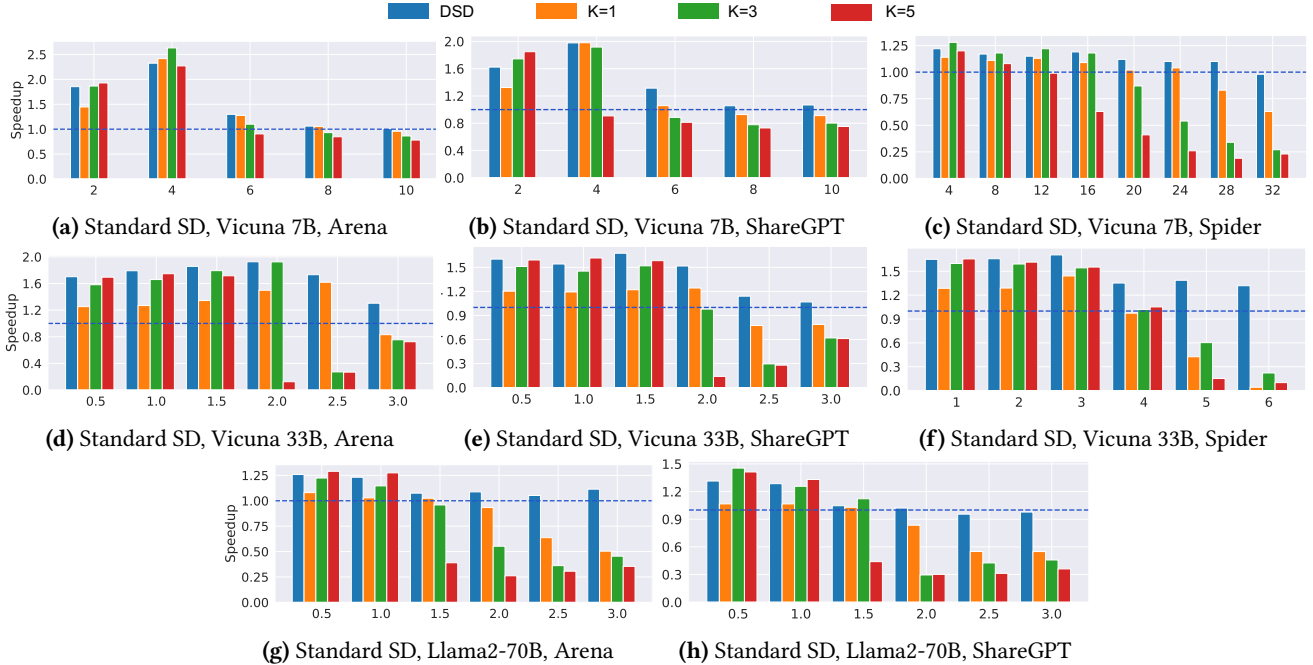


Figure 11. Latency Measurement on standard SD: Speedup across different datasets. X-axis: request rate.

speculative decoding will not compromise system performance.

7.1.2 Draft model free speculative decoding. We next evaluate the efficiency of SmartSpec with prompt lookup decoding. Like our tests with draft-model-based speculative decoding, we compare SmartSpec using fixed proposal lengths of 1, 3, and 5, against the baseline of no speculative decoding. As shown in Fig. 12, SmartSpec consistently achieves the best speedup. Notably, prompt lookup decoding with Mistral-7B (Fig. 12 (a) and (b)) shows substantial speedup even with a relatively low token acceptance rate (the measured token acceptance rate on those two settings is between 0.3 and 0.4). Unlike scenarios involving a draft model, prompt lookup does not incur significant overhead for proposing tokens, leading to notable speed gains even with lower speculative accuracy.

Like draft model-based speculative decoding, SmartSpec does not compromise performance even when the request rate is high. This is because SmartSpec adopts a conservative approach under high request rates, minimizing the wasteful computation of verifying incorrect tokens. This strategy ensures that SmartSpec maintains its efficiency across varying system loads.

7.2 Simulation Experiments

We conduct the following experiments using a simulator for several reasons. First, efficiently integrating speculative decoding into a real-world system poses a substantial engineering challenge. For instance, devising an effective verification

kernel for tree-structured speculative decoding proves difficult. The absence of such a kernel negates the advantages of speculative decoding. Additionally, we aim to explore how the system behaves under various models, workloads, and resource configurations. In particular, we are interested in assessing how the accuracy of token acceptance prediction affects overall performance. Moreover, carrying out comprehensive experiments across all possible configurations is both time-consuming and cost-prohibitive. Consequently, we utilize a simulator for all subsequent experiments.

Simulator construction. The design of the simulator is closely aligned with the operational flow of vLLM [19], accurately replicating its model scheduling and control logic. The primary distinction between the simulator and actual hardware lies in its use of an event clock to simulate kernel execution times, allowing it to operate efficiently on CPUs without the need for real GPU hardware. Essentially, the simulator employs an event clock to replace all kernel execution times while preserving all other operational logic. To ensure the event clock advances accurately and reflects realistic execution times, we have profiled GPU execution times across various hardware configurations and model settings utilized in the experiments. This approach allows us to simulate real-world operations with high fidelity.

Simulator fidelity. The data we have collected for each job allows our simulator to accurately model several system effects. This includes the performance impact of various scheduling policies and system overheads such as slow sampling and Python overhead, identified through profiling. However,

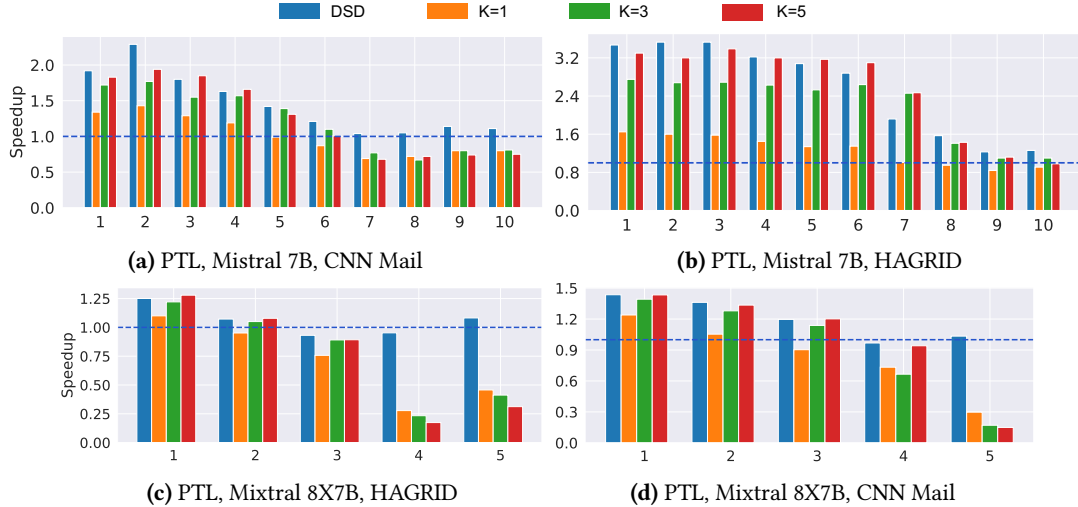


Figure 12. Latency Measurement on PTL: Speedup across different datasets. X-axis: request rate.

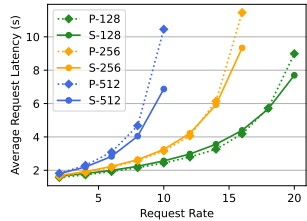


Figure 13. Simulator Fidelity. This experiment was conducted on a single Azure NC24ads machine equipped with an A100-80G GPU. The labels ‘P’ and ‘S’ indicate profiled and simulated data, respectively. The figure demonstrates that the simulated average request latency closely mirrors the measured latency across various input/output lengths and request rates.

our simulator does not account for network latency. After calibration, as shown in Fig. 13, the simulator demonstrates an error rate below 10% when the request rate is lower than the service rate. This accuracy is consistent across various input/output lengths and request rates. It is important to note that the simulator tends to under-predict latency when the request rate exceeds the service rate due to its limited ability to simulate queuing delays. For the subsequent experiments presented in this paper, we will focus exclusively on scenarios where the request rate is less than the service rate.

Using the simulator, we initially identify the discrepancy between the current speedup and the optimal speedup, where "optimal" implies foreknowledge of the accepted length. Subsequently, we implement tree-style speculative decoding Medusa with continuous batching to test SmartSpec’s generality.

7.2.1 Accepted Length Prediction and Speedup In this section, we explore how the accuracy of acceptance modeling

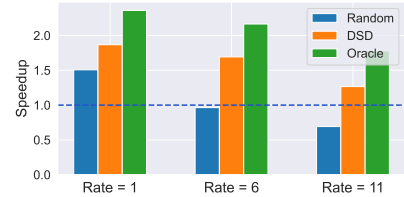


Figure 14. Optimal speedup vs SmartSpec speedup. SmartSpec means we use moving average to predict the goodput and use goodput to guide the decision. Random all means we randomly predict the accepted length without using goodput.

impacts computational speedup. We keep the request rate constant to ensure a controlled comparison of different acceptance prediction techniques. We assess the effectiveness of SmartSpec’s accepted length prediction, which employs a moving average based on historical token acceptance rates, and compare it to an oracle. This oracle assumes access to a perfect predictor and uses the actual accepted lengths to calculate goodput and determine the optimal proposed length. As shown in Figure 14, there is a noticeable performance gap between SmartSpec’s speedup and that of the oracle. Developing a more efficient accepted length predictor remains an area for future research. However, it is important to note that, even with the moving average approach, the speedup achieved by SmartSpec is substantial and represents a significant improvement over strategies that rely on random proposals.

7.2.2 Tree-style Speculative Decoding In this section, we evaluate the applicability of SmartSpec to Medusa [4], a tree-style speculative decoding method. Prior to integrating SmartSpec, Medusa could only be implemented with a

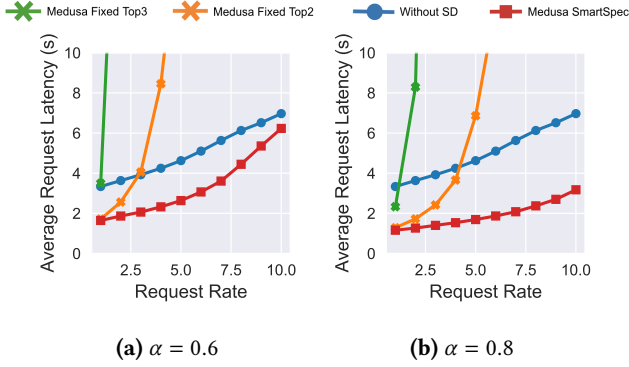
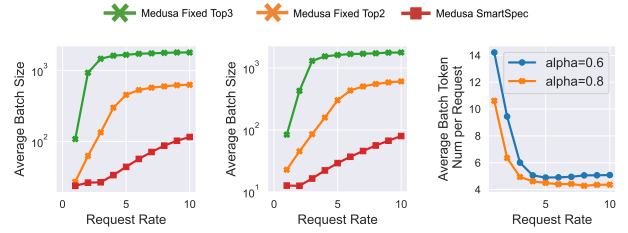


Figure 15. Average request latency of Medusa with fixed top k values and SmartSpec: Simulating the performance of Llama-7B with three fixed heads across 500 randomly sampled requests of varying input/output lengths under different request rates. α : token acceptance rate of candidate tokens across all heads.

batch size of 1. To test the enhanced capabilities, we simulate Medusa with continuous batching and assess its performance both with and without SmartSpec integration. For our experiments, we maintain a consistent token acceptance rate across all Medusa heads and for all tokens within the top-k selection. Additionally, we model Medusa with dense connectivity, ensuring that each of the top-k nodes is linked to the corresponding top-k tokens at the subsequent position.

We illustrate the average request latency across various k-values under differing token acceptance rates in Fig. 16. As demonstrated in the figure, the tree-style speculative decoding method substantially increases request latency at high request rates. This outcome aligns with expectations outlined in [4], which describes how dense connections among different heads greatly increase the the number of batched tokens. As shown in Figs. 16a and 16b, fixed top2/top3 Medusa quickly explode the batch size. Specifically, the number of batched tokens per request is represented by $\sum_{h=1}^H \prod_{i=1}^h s_i$, where s_i denotes the number of tokens sampled by head i . For example, selecting 3, 2, and 2 tokens for heads 1, 2, and 3, respectively, results in the addition of 21 tokens in the next batch for verification (calculated as $3 + 3 \times 2 + 3 \times 2 \times 2$). Conversely, with only three heads corresponding to three positions, for each request, a maximum of 4 tokens (3 plus 1 bonus token) can be processed in a single forward pass. This inefficiency underscores the need for future advancements such as those proposed by sequoia [6], which aims to develop a more structured verification tree to effectively prune less likely candidates under high request volumes.

Finally, we show the performance of SmartSpec when integrated with Medusa. We model the accepted token length as outlined in Section 4.4 and evaluate performance using goodput to decide the number of sampled tokens per head.



(a) $\alpha = 0.8$, average **(b)** $\alpha = 0.6$, average **(c)** Average token batch token number. batch token number. number per request.

Figure 16. (a), (b) show the average batch token number across batches with vanilla Medusa and SmartSpec Medusa. (c) shows the average token number across requests with SmartSpec.

As illustrated in Figure 16, SmartSpec effectively maintains manageable request latencies even under high request rates. Additionally, we depict the average number of tokens per request in Figure 16c. In both scenarios (α is 0.6 or 0.8), SmartSpec quickly reverts to top-1 sampling. It is noteworthy that the average number of batched tokens approximates to four; this consists of one input token plus one sampled token per head. Given that there are three Medusa heads, the total number of batched tokens per request remains four when employing top-1 sampling for each head.

8 Related Work

Aside from speculative decoding (Sec 2.1) and continuous batching (Sec 2.2), the system community has proposed many orthogonal methods to improve LLM inference performance.

Quantization Methods. Works like (LLM.int8() [7], GPTQ [9], Marlin [8], AWQ [23], SqueezeLLM [17]) bring down the latency of the LLM inference by using lower precision data types such as 2/3/4/6/8 bit integers. GPUs For example, a single A100 GPU can support 624 Teraops of INT8 computation through its tensor core, while only able to support 312 TFLOPS for FLOAT16. However, this class of method trade off accuracy for performance and commonly requires a calibration step. In the context of SmartSpec, quantization optimizations can be applied to both draft and target models to further improve our performance.

Prefix Caching techniques save compute of commonly repeated prefixes across requests. Systems like SGLang [45], Cascade Inference [40], and Hydragen [15] proposes efficient GPU kernels to compute and cache the computation for shared prefixes across request and deliver lower inference latency. In the context of SmartSpec, prefix caching can be applied to both draft and target workers.

9 Conclusion

Speculative decoding has recently emerged as a means to reduce inference latency at the cost of increased computational overhead. To harness the benefits of speculative decoding without compromising efficiency, we introduce an adaptive decision-making framework SmartSpec guided by the concept of goodput. Our evaluation across three distinct datasets show that SmartSpec can reduce latency by a factor of 1.2× to 3.2× when request rates are low, while sustaining performance levels even under high request rates.

References

- [1] Josh Achiam, Steven Adler, Sandhini Agarwal, Lama Ahmad, Ilge Akkaya, Florencia Leoni Aleman, Diogo Almeida, Janko Alvenschmidt, Sam Altman, Shyamal Anadkat, et al. 2023. Gpt-4 technical report. *arXiv preprint arXiv:2303.08774* (2023).
- [2] anon8231489123. 2024. *ShareGPT dataset*. https://huggingface.co/datasets/anon8231489123/ShareGPT_Vicuna_unfiltered
- [3] Yoshua Bengio, Réjean Ducharme, and Pascal Vincent. 2000. A neural probabilistic language model. *Advances in neural information processing systems* 13 (2000).
- [4] Tianle Cai, Yuhong Li, Zhengyang Geng, Hongwu Peng, Jason D Lee, Deming Chen, and Tri Dao. 2024. Medusa: Simple llm inference acceleration framework with multiple decoding heads. *arXiv preprint arXiv:2401.10774* (2024).
- [5] Charlie Chen, Sebastian Borgeaud, Geoffrey Irving, Jean-Baptiste Lespiau, Laurent Sifre, and John Jumper. 2023. Accelerating large language model decoding with speculative sampling. *arXiv preprint arXiv:2302.01318* (2023).
- [6] Zhuoming Chen, Avner May, Ruslan Svirschevski, Yuhsun Huang, Max Ryabinin, Zhihao Jia, and Beidi Chen. 2024. Sequoia: Scalable, Robust, and Hardware-aware Speculative Decoding. *arXiv preprint arXiv:2402.12374* (2024).
- [7] Tim Dettmers, Mike Lewis, Younes Belkada, and Luke Zettlemoyer. 2022. LLM.int8(): 8-bit Matrix Multiplication for Transformers at Scale. *arXiv:2208.07339* [cs.LG]
- [8] Elias Frantar and Dan Alistarh. 2024. Marlin: a fast 4-bit inference kernel for medium batchsizes. <https://github.com/IST-DASLab/marlin>.
- [9] Elias Frantar, Saleh Ashkboos, Torsten Hoefler, and Dan Alistarh. 2023. GPTQ: Accurate Post-Training Quantization for Generative Pre-trained Transformers. *arXiv:2210.17323* [cs.LG]
- [10] Yichao Fu, Peter Bailis, Ion Stoica, and Hao Zhang. 2024. Break the sequential dependency of llm inference using lookahead decoding. *arXiv preprint arXiv:2402.02057* (2024).
- [11] Pin Gao, Lingfan Yu, Yongwei Wu, and Jinyang Li. 2018. Low latency rnn inference with cellular batching. In *Proceedings of the Thirteenth EuroSys Conference*. 1–15.
- [12] Karl Moritz Hermann, Tomáš Kociský, Edward Grefenstette, Lasse Espeholt, Will Kay, Mustafa Suleyman, and Phil Blunsom. 2015. Teaching Machines to Read and Comprehend. In *NIPS*. 1693–1701. <http://papers.nips.cc/paper/5945-teaching-machines-to-read-and-comprehend>
- [13] Albert Q Jiang, Alexandre Sablayrolles, Arthur Mensch, Chris Bamford, Devendra Singh Chaplot, Diego de las Casas, Florian Bressand, Gianna Lengyel, Guillaume Lample, Lucile Saulnier, et al. 2023. Mistral 7B. *arXiv preprint arXiv:2310.06825* (2023).
- [14] Albert Q Jiang, Alexandre Sablayrolles, Antoine Roux, Arthur Mensch, Blanche Savary, Chris Bamford, Devendra Singh Chaplot, Diego de las Casas, Emma Bou Hanna, Florian Bressand, et al. 2024. Mixtral of experts. *arXiv preprint arXiv:2401.04088* (2024).
- [15] Jordan Juravsky, Bradley Brown, Ryan Ehrlich, Daniel Y. Fu, Christopher Ré, and Azalia Mirhoseini. 2024. Hydragen: High-Throughput LLM Inference with Shared Prefixes. *arXiv:2402.05099* [cs.LG]
- [16] Ehsan Kamalloo, Aref Jafari, Xinyu Zhang, Nandan Thakur, and Jimmy Lin. 2023. HAGRID: A Human-LLM Collaborative Dataset for Generative Information-Seeking with Attribution. *arXiv:2307.16883* (2023).
- [17] Sehoon Kim, Coleman Hooper, Amir Gholami, Zhen Dong, Xiyu Li, Sheng Shen, Michael W. Mahoney, and Kurt Keutzer. 2024. SqueezeLLM: Dense-and-Sparse Quantization. *arXiv:2306.07629* [cs.CL]
- [18] Sehoon Kim, Karttikeya Mangalam, Suhong Moon, Jitendra Malik, Michael W Mahoney, Amir Gholami, and Kurt Keutzer. 2024. Speculative decoding with big little decoder. *Advances in Neural Information Processing Systems* 36 (2024).
- [19] Woosuk Kwon, Zhuohan Li, Siyuan Zhuang, Ying Sheng, Lianmin Zheng, Cody Hao Yu, Joseph Gonzalez, Hao Zhang, and Ion Stoica.

2023. Efficient memory management for large language model serving with pagedattention. In *Proceedings of the 29th Symposium on Operating Systems Principles*. 611–626.
- [20] Yaniv Leviathan, Matan Kalman, and Yossi Matias. 2023. Fast inference from transformers via speculative decoding. In *International Conference on Machine Learning*. PMLR, 19274–19286.
- [21] Yuhui Li, Fangyun Wei, Chao Zhang, and Hongyang Zhang. 2024. Eagle: Speculative sampling requires rethinking feature uncertainty. *arXiv preprint arXiv:2401.15077* (2024).
- [22] Feng Lin, Hanling Yi, Hongbin Li, Yifan Yang, Xiaotian Yu, Guangming Lu, and Rong Xiao. 2024. BiTA: Bi-Directional Tuning for Lossless Acceleration in Large Language Models. *arXiv preprint arXiv:2401.12522* (2024).
- [23] Ji Lin, Jiaming Tang, Haotian Tang, Shang Yang, Xingyu Dang, Chuang Gan, and Song Han. 2023. AWQ: Activation-aware Weight Quantization for LLM Compression and Acceleration. *arXiv:2306.00978* [cs.CL]
- [24] Xiaoxuan Liu, Lanxiang Hu, Peter Bailis, Ion Stoica, Zhijie Deng, Alvin Cheung, and Hao Zhang. 2023. Online speculative decoding. *arXiv preprint arXiv:2310.07177* (2023).
- [25] Yusuf Mehdi. 2023. *Reinventing search with a new AI-powered Microsoft Bing and Edge, your copilot for the web*. <https://blogs.microsoft.com/blog/2023/02/07/reinventing-search-with-a-new-ai-powered-microsoft-bing-and-edge-your-copilot-for-the-web/> Accessed: 2024-02-21.
- [26] Xupeng Miao, Gabriele Oliaro, Zhihao Zhang, Xinhao Cheng, Zeyu Wang, Rae Ying Yee Wong, Zhuoming Chen, Daiyaan Arfeen, Reyna Abhyankar, and Zhihao Jia. 2023. Specinfer: Accelerating generative llm serving with speculative inference and token tree verification. *arXiv preprint arXiv:2305.09781* (2023).
- [27] Microsoft. 2023. *Copilot*. <https://copilot.microsoft.com/> Accessed: 2024-02-21.
- [28] Nvidia. 2024. A100 GPU Spec. <https://www.nvidia.com/en-us/data-center/a100/> Accessed: 2024-03-10.
- [29] NVIDIA. 2024. TensorRT-LLM. <https://github.com/NVIDIA/TensorRT-LLM>.
- [30] OpenAI. 2022. *ChatGPT*. <https://chat.openai.com/> Accessed: 2024-02-21.
- [31] Reiner Pope, Sholto Douglas, Aakanksha Chowdhery, Jacob Devlin, James Bradbury, Jonathan Heek, Kefan Xiao, Shivani Agrawal, and Jeff Dean. 2023. Efficiently scaling transformer inference. *Proceedings of Machine Learning and Systems* 5 (2023).
- [32] Elizabeth Reid. 2023. *Supercharging Search with generative AI*. <https://blog.google/products/search/generative-ai-search/> Accessed: 2024-02-21.
- [33] Apoorv Saxena. 2023. Prompt Lookup Decoding. <https://github.com/apoorvumang/prompt-lookup-decoding/>
- [34] Abigail See, Peter J. Liu, and Christopher D. Manning. 2017. Get To The Point: Summarization with Pointer-Generator Networks. In *Proceedings of the 55th Annual Meeting of the Association for Computational Linguistics (Volume 1: Long Papers)*. Association for Computational Linguistics, Vancouver, Canada, 1073–1083. <https://doi.org/10.18653/v1/P17-1099>
- [35] Qidong Su, Christina Giannoula, and Gennady Pekhimenko. 2023. The synergy of speculative decoding and batching in serving large language models. *arXiv preprint arXiv:2310.18813* (2023).
- [36] Hugo Touvron, Louis Martin, Kevin Stone, Peter Albert, Amjad Almahairi, Yasmine Babaei, Nikolay Bashlykov, Soumya Batra, Prajwal Bhargava, Shruti Bhosale, et al. 2023. Llama 2: Open foundation and fine-tuned chat models. *arXiv preprint arXiv:2307.09288* (2023).
- [37] Siqi Wang, Hailong Yang, Xuezhu Wang, Tongxuan Liu, Pengbo Wang, Xuning Liang, Kejie Ma, Tianyu Feng, Xin You, Yongjun Bao, et al. 2024. Minions: Accelerating Large Language Model Inference with Adaptive and Collective Speculative Decoding. *arXiv preprint arXiv:2402.15678* (2024).
- [38] Qingyun Wu, Gagan Bansal, Jieyu Zhang, Yiran Wu, Beibin Li, Erkang Zhu, Li Jiang, Xiaoyun Zhang, Shaokun Zhang, Jiale Liu, Ahmed Hassan Awadallah, Ryen W White, Doug Burger, and Chi Wang. 2023. AutoGen: Enabling Next-Gen LLM Applications via Multi-Agent Conversation. *arXiv:2308.08155* [cs.AI]
- [39] Yiran Wu, Feiran Jia, Shaokun Zhang, Hangyu Li, Erkang Zhu, Yue Wang, Yin Tat Lee, Richard Peng, Qingyun Wu, and Chi Wang. 2023. An Empirical Study on Challenging Math Problem Solving with GPT-4. In *ArXiv preprint arXiv:2306.01337*.
- [40] Zihao Ye, Ruihang Lai, Bo-Ru Lu, Chien-Yu Lin, Size Zheng, Lequn Chen, Tianqi Chen, and Luis Ceze. 2024. Cascade Inference: Memory Bandwidth Efficient Shared Prefix Batch Decoding. <https://flashinfer.ai/2024/02/02/cascade-inference.html>
- [41] Gyeong-In Yu, Joo Seong Jeong, Geon-Woo Kim, Soojeong Kim, and Byung-Gon Chun. 2022. Orca: A distributed serving system for {Transformer-Based} generative models. In *16th USENIX Symposium on Operating Systems Design and Implementation (OSDI 22)*. 521–538.
- [42] Tao Yu, Rui Zhang, Kai Yang, Michihiro Yasunaga, Dongxu Wang, Zifan Li, James Ma, Irene Li, Qingning Yao, Shanelle Roman, et al. 2018. Spider: A large-scale human-labeled dataset for complex and cross-domain semantic parsing and text-to-sql task. *arXiv preprint arXiv:1809.08887* (2018).
- [43] Jun Zhang, Jue Wang, Huan Li, Lidan Shou, Ke Chen, Gang Chen, and Sharad Mehrotra. 2023. Draft & verify: Lossless large language model acceleration via self-speculative decoding. *arXiv preprint arXiv:2309.08168* (2023).
- [44] Lianmin Zheng, Wei-Lin Chiang, Ying Sheng, Siyuan Zhuang, Zhanghao Wu, Yonghao Zhuang, Zi Lin, Zhuohan Li, Dacheng Li, Eric Xing, et al. 2024. Judging llm-as-a-judge with mt-bench and chatbot arena. *Advances in Neural Information Processing Systems* 36 (2024).
- [45] Lianmin Zheng, Liangsheng Yin, Zhiqiang Xie, Jeff Huang, Chuyue Sun, Cody Hao Yu, Shiyi Cao, Christos Kozyrakis, Ion Stoica, Joseph E. Gonzalez, Clark Barrett, and Ying Sheng. 2023. Efficiently Programming Large Language Models using SGLang. *arXiv:2312.07104* [cs.AI]
- [46] Yongchao Zhou, Kaifeng Lyu, Ankit Singh Rawat, Aditya Krishna Menon, Afshin Rostamizadeh, Sanjiv Kumar, Jean-François Kagy, and Rishabh Agarwal. 2023. Distillspec: Improving speculative decoding via knowledge distillation. *arXiv preprint arXiv:2310.08461* (2023).

Algorithm 3 SmartSpec confidence based propose and verify.

Require: Pending requests R . Confidence threshold T . Max propose length P .

- 1: $best_goodput, best_verify_lens \leftarrow -1, 0$
- 2: **for** each r in R **do**
- 3: // Initialize the confidence before proposing the first token for each request
- 4: $r.conf = 1$
- 5: **end for**
- 6: $propose_steps \leftarrow 0$
- 7: **while** $len(R) > 0$ and $propose_steps \leq P$ **do**
- 8: $R' = \{r \text{ for } r \text{ in } R \text{ if } r.conf > T\}$
- 9: // Propose will update the $conf$ attribute for each request r in R'
- 10: $R = \text{Propose}(R')$
- 11: $propose_steps++$
- 12: **end while**
- 13: $\text{ArgmaxGoodput}(R)$
- 14: $\text{Score}(R)$

10 Appendix

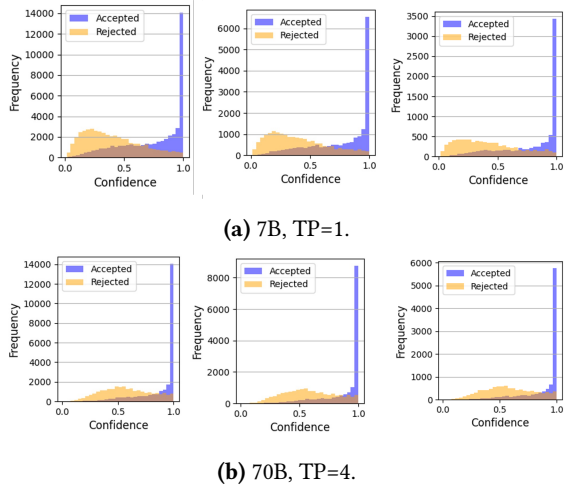


Figure 17. Confidence distribution.

In this section, we explore the utilization of confidence as a criterion for token acceptance. Confidence is defined as the output probability of the proposed token generated by the draft model. As depicted in Figure 17, a discernible distinction exists between the confidence distributions of accepted and rejected tokens. This distinction intuitively suggests that tokens proposed by the draft model, when accompanied by high confidence levels, are likely to be accurate. Conversely, proposals made with low confidence are less likely to be accepted by the target model. In practice, we establish a threshold T . Tokens with a confidence level exceeding T are predicted to be accepted, while those below this threshold are anticipated to be rejected.

Initially, SmartSpec sets the confidence level of each request to 1, adhering to the definition in Section 4.4 where confidence is treated as a probability and thus cannot exceed 1. This ensures that the draft model will propose at least one token, activating the procedure described in lines 7-12 at least once, provided that $P > 0$. During each proposal step (lines 7-12), SmartSpec selectively processes only those requests, denoted as R' , whose confidence levels surpass the specified threshold T from the preceding proposal step. Subsequently, SmartSpec batches these R' requests for a forward pass execution. Following the strategy outlined above, SmartSpec also explores all potential lengths for verification and opts for the length that maximizes goodput.